Supporting Information

Simply translating mercury detection into a temperature measurement: using an aggregation-activated oxidase-like activity of gold nanoparticles

Pengli An,[a] HonghongRao,[b]* Min Gao,[a] Xin Xue,[a] Xiuhui Liu,[a] Xiaoquan Lu[a] and ZhonghuaXue [a]*

[a]*Key Laboratory of Bioelectrochemistry & Environmental Analysis of Gansu Province, College of Chemistry & Chemical Engineering, Northwest Normal University, Lanzhou, 730070, China.*
[b]*School of chemistry & Chemical Engineering, Lanzhou City University, Lanzhou, 730070, China.*
**Tel/Fax: +86 931 7970520: E-mail: xzh@nwnu.edu.cn; rhh@nwnu.edu.cn*
Electronic Supplementary Information (ESI) available: See DOI: 10.1039/x0xx0x Address here.

Experimental Section

Material and reagent: Chloroauric acid tetrahydrate ($HAuCl_4 \cdot 4H_2O$), and β-cyclodextrin (β-CD), mercury nitrate ($Hg(NO_3)_2$), 3,3',5,5'-tetramethylbenzidine (TMB), sodium azide (NaN_3), tertiary butanol (*t*-BuOH), mannitol, sodium bicarbonate ($NaHCO_3$), and ethanol (CH_2OH) were purchased from Sinopharm Chemical Reagent (Shanghai, China). Superoxide dismutase (SOD) from baker's yeast (S. cerevisiae) was purchased from Sigma-Aldrich Company (Shanghai, China). The Hg^{2+} standard solution was purchased from Guobiao (Beijing) Testing & Certification Co., Ltd. Human blood specimens gained from Hospital 940 of PLA Joint Logistics Support Force (Gansu, China). All reagents were of analytical grade and without any further purification. All aqueous solutions used in this experiment were prepared with Milli-Q ultrapure water (18.2 $M\Omega \cdot cm^{-1}$).

Instrumentation: The transmission electron microscopy (TEM), elemental mapping and EDS was obtained via a FEI Tecnai F20 (200 kV) instrument. The UV–vis spectra were performed on a T6 new century spectrophotometer (China). Fourier transform infrared spectra (FTIR) were carried out on a FTS3000 FTIR instrument in the ranged from 400 to 4000 cm^{-1}. A diode laser (MDL-H-808-5W-17120005) was purchased from Changchun New Industries Optoelectronics Technology Co., Ltd. A pen-style digital thermometer (MITIR-TP677) was obtained from a local supermarket. The concentration of Hg^{2+} in real samples was measured through ICP-MS Spectrometer (NexION 350D, PerkinElmer, US). Color photographs of the solutions were recorded by Canon camera (EOS-70D). Centrifugation was performed on a Ke Cheng H3-18K centrifuge.

Preparation of AuNPs@β-CD: According to the previous report,[1] the AuNPs@β-CD were

successfully synthesized. The Milli-Q water (105 mL) mixed with 15 mL of PBS (pH 7.0) buffer solution, 30 mL of β-CD (0.01 M) and 309 μL of $HAuCl_4 \cdot 4H_2O$ (0.1 M) solutions, then was added under vigorous stirring. The yellowish mixed solution was heated to reflux within an hour. After that, a color change from yellowish, gray violet, and pink to wine red was observed, indicating the successful formation of AuNPs@β-CD. The wine-red AuNPs@β-CD were removed by centrifugation and re-dispersed in 16 mL Milli-Q water. Finally, the as-received AuNPs@β-CD were stored at 4 °C. The concentration of the AuNPs@β-CD was calculated as the reported works.[2, 3] They explored a method for calculating the particle size (*d*) from the UV-vis spectrum, and established the method to obtain the AuNPs concentration (*c*) based on relationship analysis between the extinction efficiency (Qext) and *d* of AuNPs. Specifically, an equation was used to calculate AuNPs concentration (*c*, in mol per litre) from the absorption *A* at 450 nm for a standard path length l of 1 cm. The data of the molar decadic extinction coefficient (ε) with the different *d* can be obtained by checking the data sheet. Based on this, the concentration of the prepared AuNPs@β-CD with 30 nm in this work can be approximately calculated according to the following equation:

$$c = A_{450}/\varepsilon_{450}$$

Where the ε_{450} of 30 nm AuNPs is 1.96E+09 $M^{-1} \cdot cm^{-1}$ and the absorbance (A_{450}) of the AuNPs@β-CD at 450 nm was measured with the path length l of the UV-vis spectrometer of 1 cm.

Condition Optimization: To gain an excellent photothermometric sensing performance of Hg^{2+}, experiment conditions containing reaction temperature and time, AuNPs@β-CD and TMB concentration were optimized by using Vis−NIR spectra, respectively. In the photothermometric testing, an 808 nm diode laser was used to irradiate reaction solutions. For the optimization of the irradiation power and time, the temperature was recorded using a common pen-style digital thermometer upon the continuous laser irradiation from 10 s and up to 240 s. The position of the thermometer was fixed in all temperature measurements to avoid temperature variations from position to position.

Photothermometric assay of Hg^{2+}: For photothermometric assay, the reaction solutions were irradiated by an 808 nm laser for 240 s with a power of 4.5 W**,** and the corresponding temperature changes were measured by using a pen-style digital thermometer. The calibration plot of the photothermometric detection was assessed according to the equation:

$$\Delta T = T - T_0$$

Where ΔT is the temperature increment, T and T_0 are defined as the temperatures of reaction

solution before and after laser irradiation, respectively.

Colorimetric assay of Hg^{2+}: Colorimetric detection of Hg^{2+} was carried out according to the following procedure: under the optimized conditions, 20 μL of Hg^{2+} solutions with different concentrations were added into 1855 μL aqueous solution containing 500 μM TMB and 25 μL AuNPs@β-CD, and then reacted for 2 min at room temperature. Finally, the Vis-NIR absorption spectra of the mixture solution were recorded in the range from 400 nm to 1000 nm. Finally, the calibration plot of the colorimetric assay was evaluated by *A,* which was the absorbance of TMBox at 652 nm in the reaction solutions.

Selectivity of Hg^{2+} sensing: Under the optimal conditions, the selectivity of the proposed photothermometric and colorimetric Hg^{2+} analysis was assessed by adding different interferences, including Na^{+}, K^{+}, Mg^{2+}, Bi^{3+}, Ca^{2+},Mn^{2+}, Co^{2+}, Ni^{2+}, Al^{3+}, Cd^{2+}, Ag^{+}, Cu^{2+}, Fe^{2+}, Fe^{3+}, Cr^{3+}, Ba^{2+}, Ce^{3+}, Pb^{2+}, Zn^{2+}, NH_4^{+}, OH^{-}, Ac^{-}, NO_3^{-}, CO_3^{2-}, SO_4^{2-}, PO_4^{3-}, HCO_3^{-}, $H_2PO_4^{-}$, HPO_4^{2-}, PPi, glucose, lactose, glycine, and sarcosine. The concentrations of all interferences were 20-fold higher than Hg^{2+} concentration (15 μM).

Analysis of real sample: Fresh human blood samples were obtained from three healthy adult volunteers at a local hospital and stored frozen until the assay. In this work, the human blood sample was firstly digested for detecting Hg^{2+} in the blood followed the procedure reported earlier.[4] 1 mL of blood samples was diluted with 8 mL Milli-Q water and then treated with 1 mL of HNO_3 for 4 h. The sample was briefly centrifuged at 4000 rpm for 2 min. The supernatant was diluted with Milli-Q water and neutralized with 1 M NaOH solution. Then the treated blood sample was subjected to direct detection. All the experiments were performed in compliance with the relevant laws and institutional guidelines, and approved by the relevant institutional committees (Ethics Committee of China Pharmaceutical University). Finally, the evaluation of Hg^{2+} levels in human blood was performed with the same operations that used in photothermometric and colorimetric tests, in which the samples of Hg^{2+} were prepared by spiking different concentrations of Hg^{2+} in real human blood samples.

Characterization of AuNPs@β-CD: In this work, the prepared AuNPs@β-CD was characterized through Vis-NIR, Energy Dispersive spectroscopy (EDS), FT-IR spectroscopy (FT-IR), and X-ray photoelectron spectroscopy (XPS). As shown in Fig. S1 A, the Vis-NIR spectrum of wine-red AuNPs@β-CD solution showed the characteristic absorption peak of gold nanoparticles at 520 nm. Then, EDS and XPS survey spectra confirmed the presence of Au along with C, O. And the elements of C and O both belonged to the β-CD coating of AuNPs@β-CD. In the FT-IR spectroscopy, it is obvious that AuNPs@β-CD retained the main chemical function groups of β-CD molecules. The hydroxyl groups of AuNPs@β-CD decreased as the typical absorption peaks

at of hydroxy band (−OH) of β-CD became relatively broader. At the same time, β-CD reaction with $HAuCl_4$, the relative intensity of hydroxyl groups decreased but the peak of carbonyl groups appeared. In addition, the C 1s XPS spectrum exhibits four binding-energy peaks at 284.8 eV (C-C), 286.4eV (C-OH), 287.7 eV (O-C-O/C=O), and 288.6 eV (O-C-O) and O 1s XPS spectrum demonstrates three peaks at 531.7 eV (C-O), 530.4 eV (C=O), and 532.8 eV (O-C=O/C-O-C). All the results confirmed the successful preparation of AuNPs@β-CD.[5]

Optimization of the experimental conditions: To investigate the sensing performance of the proposed AuNPs@β-CD aggregation-based photothermometric platform, the Vis-NIR spectra, solution color and PTEs of the reaction systems with different Hg^{2+} concentrations were studied in detail. Firstly, some factors influencing the sensing performance were evaluated, such as buffer solution, pH, reaction temperature and time, TMB and AuNPs@β-CD content, and the power and irradiation time of 808 nm laser. A higher absorbance of TMBox (A_{652}) was observed in water at pH 7.5 (Fig. S7) and obtained at the room temperature within 2 min reaction time (Fig. S8), respectively, which were selected as the optimal pH and reaction temperature and time. In addition, by investigating the influence of the TMB and AuNPs@β-CD content on the optical and thermal response, we found that 500 μM of TMB and 25 μL of AuNPs@β-CD (A_{520}=0.075, Fig. S9) were the optimal conditions for sensing Hg^{2+}. As is well-known, since the laser irradiation power and irradiation time play a key role in the PTEs, we therefore investigated these factors on the photothermal detectability of our sensing system. As displayed in Fig. S10, the temperature response of the reaction system against different irradiation powers of 808 nm laser suggested 4.5 W as the optimal irradiation power was available. Furthermore, under the irradiation of a 4.5 W NIR laser, the system temperature increased dramatically with the increase in the AuNPs@β-CD content at different irradiation times (e.g. 60, 120, 180, 240 s) (Fig. S11). Upon the irradiation time of 240 s and 300 s, the temperature increases were proportional to the AuNPs@β-CD content in the range from 1 to 25 μL with slopes of 0.322 °C·μL^{-1} at 240 s (R2=0.992) and 0.315 °C·μL^{-1} at 300 s (R^2=0.987), respectively. Compared to the irradiation time of 300 s, the irradiation time of 240 s exhibited better linearity and a bigger slope to acquire a sensitive and time-saving temperature measurement for Hg^{2+}. Thus, the laser irradiation time of 240 s was chosen as the optimal irradiation time in the subsequent experiments.

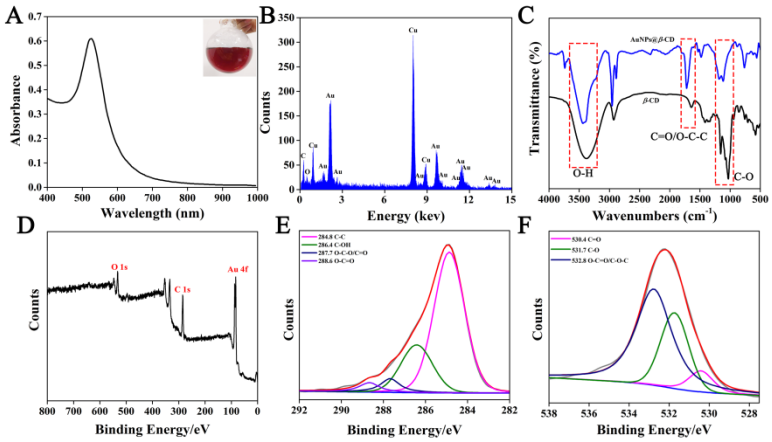

Fig. S1. Characterization of AuNPs@β-CD. (A) Vis-NIR absorption (inset: the corresponding photograph), (B) EDS, (C) FT-IR spectra. (D)XPS survey spectra, (E) XPS of the C 1s region, and (F) XPS of the O 1s region.

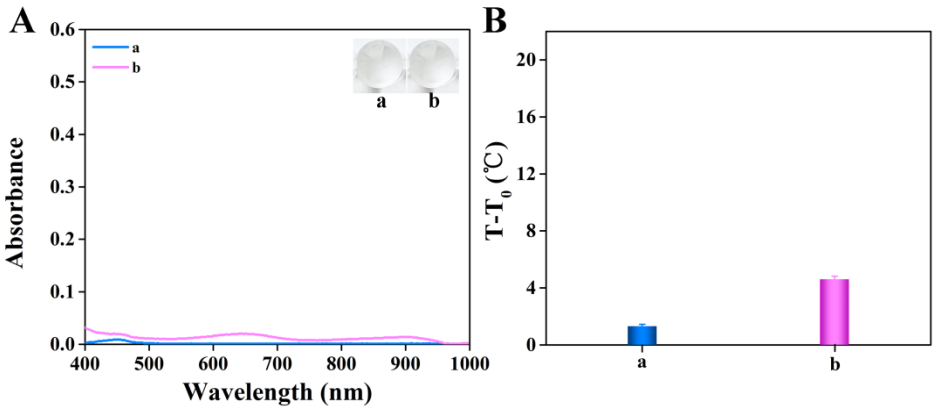

Fig. S2 (A) Vis-NIR spectra of different components at neutral pH (Insert of photographs). (B) Temperature increase (T-T_0) of reaction solution before and after irradiation with an 808 nm laser for 240 s (a: 15 μM Hg^{2+}, b: 15 μM Hg^{2+} + 500 μM TMB).

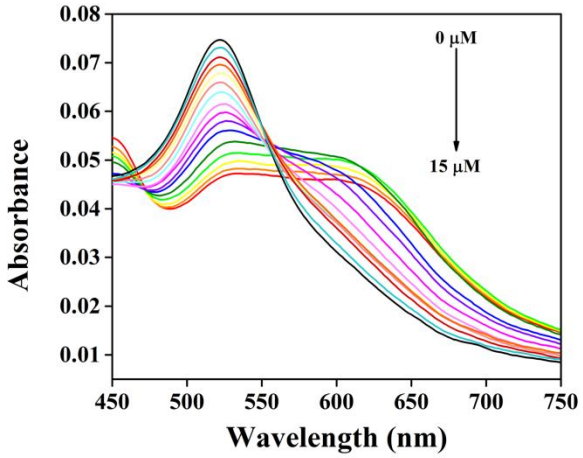

Fig. S3 Vis-NIR spectra of AuNPs@β-CD (25 μL) with different concentration of Hg^{2+} (0-15 μM) in water.

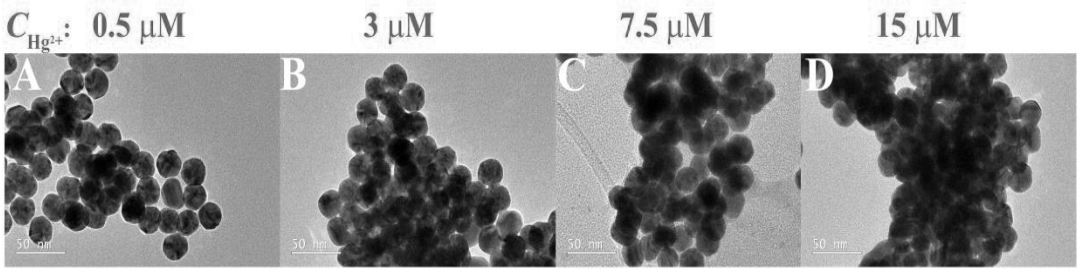

Fig. S4 (A-D) The TEM images of AuNPs@β-CD with different the concentrations of Hg^{2+} from 0.5-15 μM

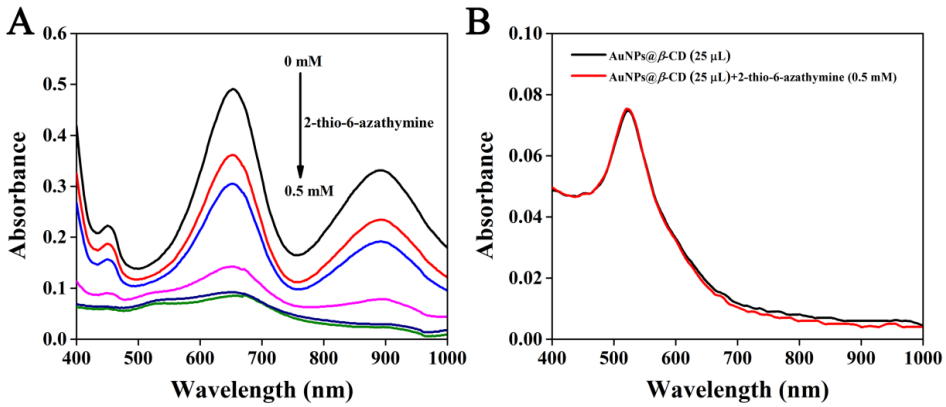

Fig. S5 Vis-NIR spectra of 500 μM TMB reaction solutions by the AuNPs@β-CD-catalyzed in the presence of 15 μM Hg^{2+} (A) at different concentrations of 2-thio-6-azathymine (0-0.5 mM). (B) Vis-NIR spectra of AuNPs@β-CD in the absence and presence of 2-thio-6-azathymine.

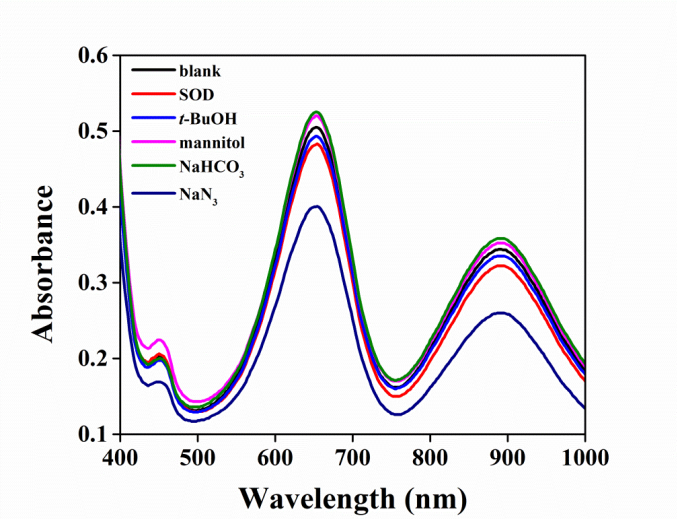

Fig. S6 Vis-NIR spectra of reaction solutions with different free-radical scavengers. The final concentrations: 10 mM SOD, 1 M *t*-BuOH, 10 mM mannitol, 10 mM $NaHCO_3$, and 10 mM NaN_3.

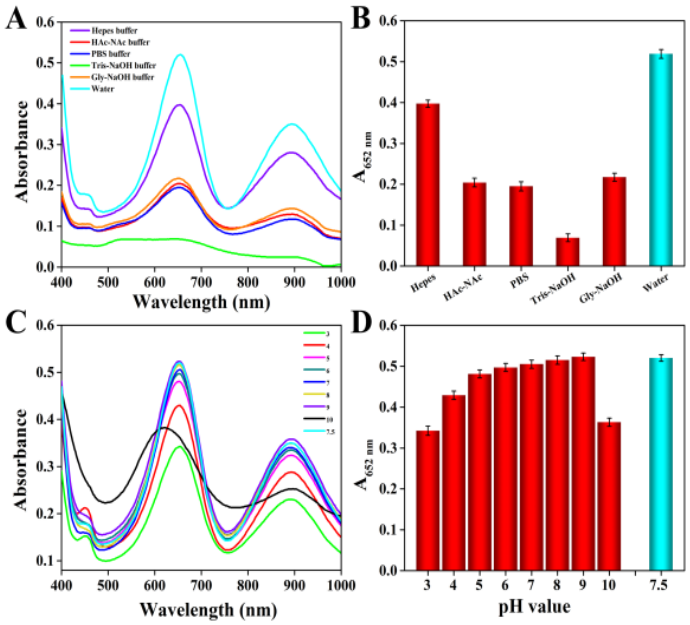

Fig. S7 Optimization of reaction condition in the proposed photothermometric system. (A) Vis-NIR absorption spectra of the different reaction solutions and (B) the plot of corresponding absorbance ($A_{652\ nm}$); (C) Vis-NIR absorption spectra of the different pH condition and (D) the plot of corresponding absorbance ($A_{652\ nm}$).

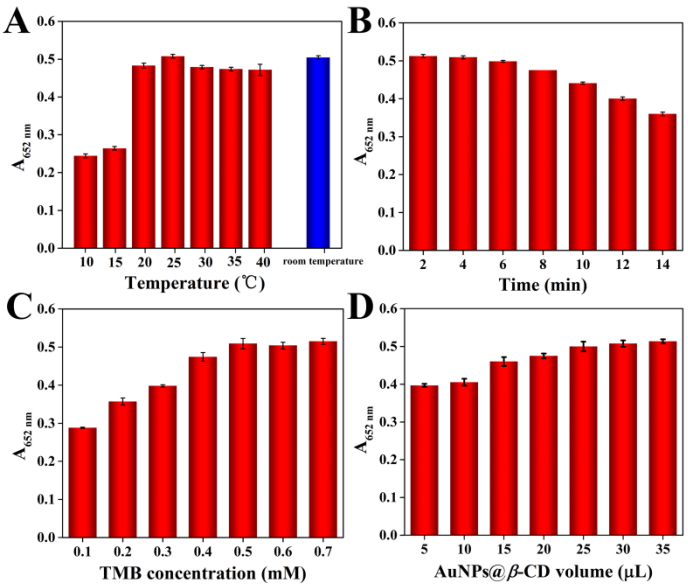

Fig. S8 Optimization of reaction condition in the proposed photothermometric system. Typical Vis-NIR absorbance ($A_{652\ nm}$) of the reaction solutions under different conditions: effect of (A) temperature, (B) time, (C) TMB concentration, and (D) AuNPs@β-CD volume.

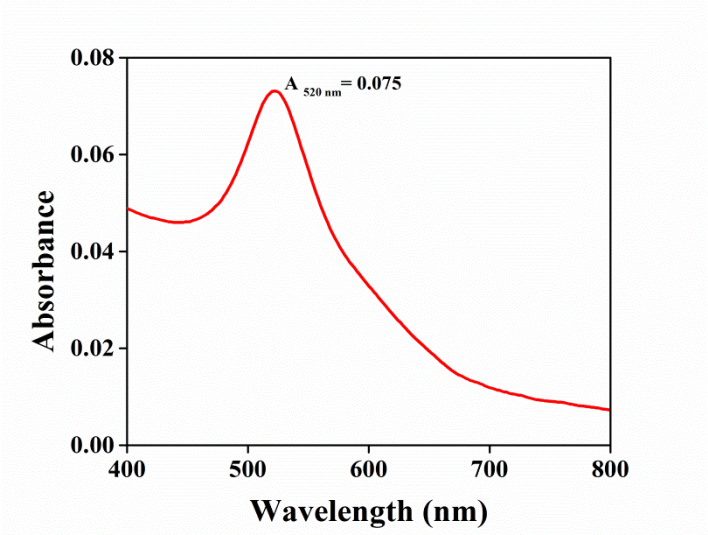

Fig. S9 The Vis-NIR spectrum of AuNPs@β-CD (25 μL) solution.

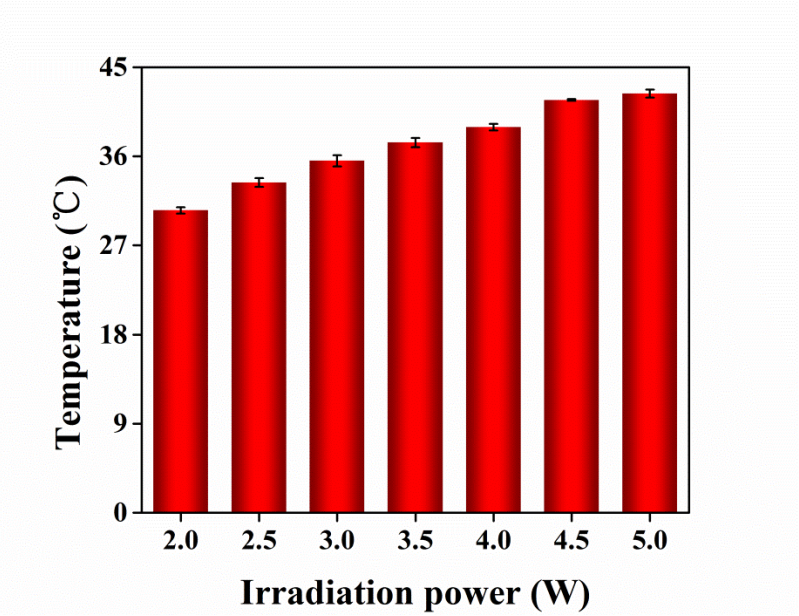

Fig. S10 Optimization of the irradiation power in the proposed photothermometric system. Temperature of the proposed photothermometric Hg^{2+} system at different irradiation power (Irradiation time: 240 s).

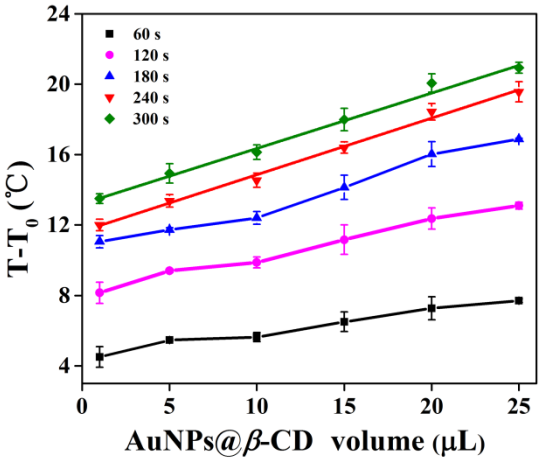

Fig. S11 Optimization of the AuNPs@β-CD content in the proposed photothermometric system. Temperature increases versus AuNPs@β-CD volume in the range of 1.0-25 μL under the 808 nm laser irradiation at a power of 4.5 W with different irradiation time (60-300s). Error bars indicate standard deviations (n=3).

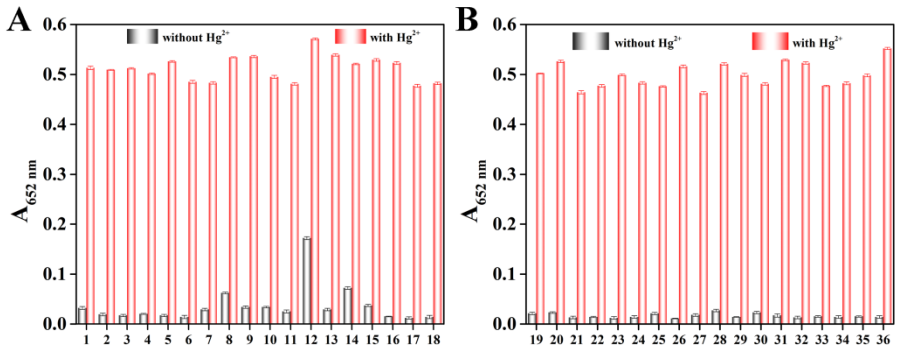

Fig. S12 Specificity test using different interferences on the colorimetric sensing platform. Absorbance at 652 nm of the reaction system with different components (A) 1-18: 1.Na^{+}; 2.K^{+}; 3.Mg^{2+}; 4.Bi^{3+}; 5.Ca^{2+}; 6.Mn^{2+};7.Co^{2+}; 8.Ni^{2+}; 9.Al^{3+}; 10.Cd^{2+}; 11. Ag^{+} + Ac^{-}; 12. Ag^{+}; 13.Cu^{2+}; 14.Fe^{2+}; 15.Fe^{3+}; 16.Cr^{3+}; 17.Ba^{2+}; 18.Ce^{3+}; (B) 19-36: 19.Pb^{2+}; 20.Zn^{2+}; 21.NH_4^{+}; 22.OH^{-}; 23.Ac^{-}; 24.NO_3^{-}; 25.CO_3^{2-}; 26.SO_4^{2-}; 27.PO_4^{3-}; 28.HCO_3^{-}; 29.$H_2PO_4^{-}$; 30.HPO_4^{2-}; 31.PPi; 32.lactose 33.glucose; 34.glycine; 35.sarcosine; 36.control in the absence and presence of Hg^{2+}. Error bars indicate standard deviations (n=3)

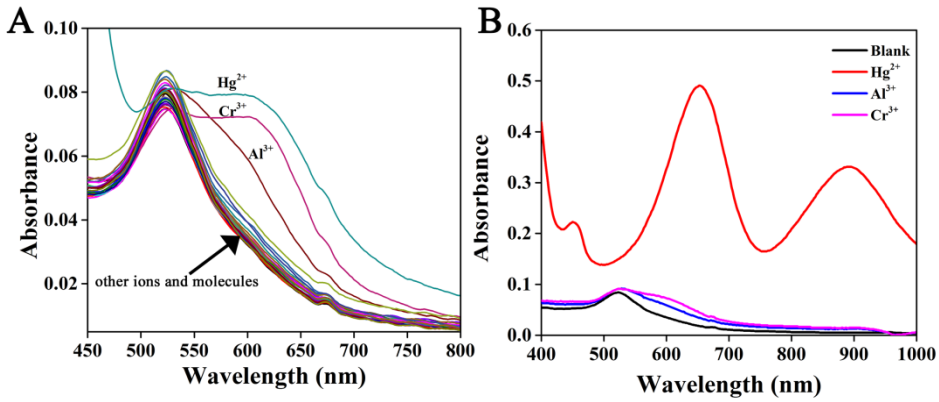

Fig. S13 (A) Vis-NIR spectra of AuNPs@β-CD with different components (Na^{+}; K^{+}; Mg^{2+}; Bi^{3+}; Ca^{2+}; Mn^{2+}; Co^{2+}; Ni^{2+}; Al^{3+}; Cd^{2+}; Ag^{+}; Cu^{2+}; Fe^{2+}; Fe^{3+}; Cr^{3+};.Ba^{2+}; Ce^{3+}; Pb^{2+}; Zn^{2+}; NH_4^{+}; OH^{-}; Ac^{-}; NO_3^{-}; CO_3^{2-}; SO_4^{2-}; PO_4^{3-}; HCO_3^{-}; $H_2PO_4^{-}$; HPO_4^{2-}; PPi; lactose; glucose; glycine , sarcosine, Hg^{2+}, blank). (B) Vis-NIR spectra of TMBox with different components containing 15 μM M^{n+} (Hg^{2+}, Al^{3+}, Cr^{3+}), 25 μL AuNPs@β-CD, and 500 μM TMB.

Table S1. Comparison of the sensing performance of different Hg^{2+} assays.

Detection Methods	Material	Linear Range	LOD	Ref.
Fluorescent	NSPCDs**	1-70 μM	0.18 μM	[6]
Fluorescent	NSPCDs	0-20 μM	0.18 μM	[7]
Fluorescent	NCDs*	1-12 μM	0.226 μM	[8]
Colorimetric	DNA/AuNPs	0-5 μM	0.5 μM	[9]
Colorimetric	Ag@GO	10-200 μM	0.338 μM	[10]
Colorimetric	AgNPs	10-100 μM	2.2 μM	[11]
Colorimetric	AuNPs@β-CD	0.4-15 μM	0.147 μM	This work
photothermometric		0.4-8 μM	0.06 μM	

Table S2. Hg^{2+} analysis in the real sample by the proposed sensing platform and ICP-MS.

Samples	Spiked /μM	Photothermometric assay		Colorimetric assay		ICP-MS	
		Found / μM	Recovery /%	Found / μM	Recovery /%	Found / μM	Recovery /%
1	0	0	-	0	-	0.001	-
2	1	0.97	96.9	1.02	101.8	1.00	99.9
3	3	3.11	103.6	2.99	99.6	2.98	99.3
4	6	6.21	103.5	6.15	102.5	6.01	100.1

Reference

1. Y. Zhao, Y. Huang, H. Zhu, Q. Zhu and Y. Xia, *J Am Chem Soc*, 2016, **138**, 16645-16654.
2. N. G. Khlebtsov, *Analytical Chemistry*, 2008, **80**, 6620-6625.
3. W. Haiss, N. T. K. Thanh, J. Aveyard and D. G. Fernig, *Analytical Chemistry*, 2007, **79**, 4215-4221.
4. Z. Zhang, W. Li, Q. Zhao, M. Cheng, L. Xu and X. Fang, *Biosens Bioelectron*, 2014, **59**, 40-44.
5. J. Li, X. Hu, Y. Zhou, L. Zhang, Z. Ge, X. Wang and W. Xu, *ACS Applied Nano Materials*, 2019, **2**, 2743-2751.
6. Y. Guo, Z. Wang, H. Shao and X. Jiang, *Carbon*, 2013, **52**, 583-589.
7. Y. Wang, S.-H. Kim and L. Feng, *Analytica Chimica Acta*, 2015, **890**, 134-142.
8. F. Yan, Y. Zou, M. Wang, X. Mu, N. Yang and L. Chen, *Sensors and Actuators B: Chemical*, 2014, **192**, 488-495.
9. X. Xu, J. Wang, K. Jiao and X. Yang, *Biosensors and Bioelectronics*, 2009, **24**, 3153-3158.
10. K. Zangeneh Kamali, A. Pandikumar, S. Jayabal, R. Ramaraj, H. N. Lim, B. H. Ong, C. S. D. Bien, Y. Y. Kee and N. M. Huang, *Microchimica Acta*, 2016, **183**, 369-377.
11. L. Chen, X. Fu, W. Lu and L. Chen, *ACS Applied Materials & Interfaces*, 2013, **5**, 284-290.